Sustainability in Environment
ISSN 2470-637X (Print) ISSN 2470-6388 (Online)
Vol. 9, No. 4, 2024
www.scholink.org/ojs/index.php/se

Original Paper

Study on The Response Characteristics of Monopile Offshore Wind Turbines under Non-Gaussian loads in Typhoons

Xiaoyu Tan[1], Jiaqi Li[1], Yuan Hu[1*], Tao Song[1], Siyi Chen[1] & Jiaxiao Li[1]

[1] Chongqing Jiaotong University, Chongqing 400060, China

[*] Hu Yuan, Chongqing Jiaotong University, Chongqing 400060, China

Received: August 23, 2024 Accepted: October 02, 2024 Online Published: October 22, 2024

doi:10.22158/se.v9n4p35 URL: http://dx.doi.org/10.22158/se.v9n4p35

Abstract

The fan structure is often seriously damaged under typhoon, so the study of the fan structure under typhoon is of great significance for its disaster prevention and mitigation. The actual measurement shows that the typhoon has obvious non-Gaussian characteristics, and the influence mechanism of this characteristic on the fan response characteristics is not clear. Therefore study the response characteristics of fans under non-Gaussian load. First, based on the autoregressive AR model, combined with the Johnson conversion model (JTM); second, the wind load is determined based on the specification; then the wind load. Finally, the response characteristics of 5MW fan are studied by characterizing the numerical cases of non-Gaussian fan with different strength of typhoon. The results show that the non-high characteristics of non-Gaussian wind field and the non-Gaussian characteristics become stronger with the strength of the non-Gaussian characteristics of wind field.

Keywords

Typhoon, non-Gaussian characteristics, wind load, fan response characteristics, autoregressive (AR) model

1. Introduction

With the extensive application of wind power generation, offshore wind turbines, as key facilities, have their stability and safety directly influencing the operational efficiency and economic benefits of wind farms (Liu et al., 2013). Nevertheless, under severe meteorological conditions such as typhoons, wind turbines face complex load conditions, and the problem of structural damage has become increasingly prominent, which has become a bottleneck in the development of the wind power industry. In the past decade, cases of wind turbine damage due to extreme weather in wind farms at home and abroad have been common. For example, in July 2018, Typhoon Maria landed in Fujian, causing damage to multiple

wind turbines in Zhongmin (Xiapu) Wind Farm; in November 2021, wind farms in Germany and France suffered severe damage during the autumn storm, with a 4.2MW wind turbine blade in Germany's Nattheim Wind Farm being twisted; in September 2024, Super Typhoon Capricorn landed in Wenchang, Hainan, and several wind turbines were uprooted, with losses amounting to hundreds of millions of yuan.

A great number of scholars have carried out investigations regarding the wind - induced response characteristics of wind turbine structures (Lobitz, 1984; Murtagh et al., 2004, 2005; Wang et al., 2013; Quan, 2002). In their research on the wind - induced response analysis and wind - vibration control of wind turbine towers, Li Bin et al. (2017) noted that the dynamic response at the top of the wind turbine tower exhibits strong randomness and volatility. Zhao Yan et al. (2018), in their research on the vibration monitoring and dynamic response of the wind turbine structure, conducted long - term monitoring on a 1.5MW wind turbine tower. They also studied the vibration response and fatigue damage of the wind turbine structure under diverse working conditions. Zhang and Wen (2013) and other researchers have performed relevant research on the dynamic response characteristics of large - scale wind turbine towers under pulsating wind.

Nevertheless, the majority of the aforementioned research is centered on Gaussian wind fields. In contrast to normal wind, typhoon wind speed clearly displays non - Gaussian characteristics. This non - Gaussian property will result in an uneven stress distribution within the wind turbine structure, which will significantly modify the dynamic response characteristics of the wind turbine and accelerate the fatigue damage of the structure. As pointed out in the article (Miao et al., 2021) "Estimation of Extreme Response of Wind Turbine Structure under Non - Gaussian Wind Field", on the basis of the Hermite moment model, according to the Kaimal spectrum, wind fields with three different probability characteristics of Gaussian, non - Gaussian hardening and softening are generated for a typical wind turbine structure in normal operation and shutdown states, and a full - life reliability analysis of the wind turbine is carried out. The dynamic response of the wind turbine is calculated from the aerodynamic model and multi - body dynamics of the blade, and the structural responses under the action of wind fields with different probability characteristics are analyzed. Consequently, it is of great urgency to conduct research on the response characteristics of wind turbine structures under typhoon non - Gaussian wind loads.

This article commences by presenting the wind turbine structure model that is adopted. Subsequently, it offers the method for determining the non - Gaussian wind loads of the wind turbine. Among these methods, the wind loads with non - Gaussian characteristics are mainly simulated based on the AR model (Wang, 2007) and the Johnson Transformation Model (JTM) (Wu, 2020). After that, research is carried out on the influence of wind loads with different intensities of non - Gaussian characteristics on the dynamic response characteristics of the wind turbine structure. Eventually, certain conclusions are drawn.

It should be emphasized that the non - Gaussian characteristics of typhoon wind loads can have far -

reaching implications for the integrity and performance of wind turbine structures. For example, the uneven stress distribution may lead to premature wear and tear in specific parts of the structure, which could potentially reduce the overall lifespan of the wind turbine. Moreover, the alteration of dynamic response characteristics might also affect the power generation efficiency of the wind turbine. If the structure is constantly subjected to abnormal vibrations due to the non - Gaussian wind loads, it may not be able to operate at its optimal capacity, thereby resulting in a decrease in energy output.

2. The Structure Model and Parameters of the Fan

At present, in China, most of the offshore wind power projects are concentrated in the shallow - sea areas close to the coastline. Due to the relatively shallow water depth and complex terrain there, the monopile foundation has become the mainstream wind turbine support structure because of its simple structure, strong adaptability and high bearing capacity. Therefore, this article takes the iconic 5 - MW monopile offshore wind turbine proposed by the National Renewable Energy Laboratory (NREL) of the United States as the research object. As a global leader in the renewable energy field, NREL's 5 - MW monopile wind turbine design scheme combines advanced technological concepts and engineering practices and has become a benchmark in the offshore wind power industry. The NREL 5 - MW wind turbine is a typical three - blade upwind variable - speed wind generator, which can efficiently utilize wind energy resources to generate clean and renewable electricity. This model is often used in the scientific research field to study problems such as the dynamic response of wind turbines. The research results are helpful for more accurately predicting the performance and safety of wind turbines in extreme weather, thus providing an important reference for the design optimization of wind turbine structures. The following are some basic parameters of the NREL 5 - MW wind turbine model.

Table 1. Basic Parameters of NREL 5MW Wind Turbine

Name	Parameter
Rated power (MW)	5
Number of blades	3
Impeller diameter, hub diameter (m)	126/3
Hub height (distance from sea level in m)	90
Single - pile diameter, tower bottom diameter, tower top diameter (m)	6/6/3.87
Cut - in wind speed, rated wind speed, cut - out wind speed (m/s)	3/11.4/25
Cut - in rotational speed, rated rotational speed (rpm)	6.9/12.1
Rotor mass, nacelle mass (t)	110/240

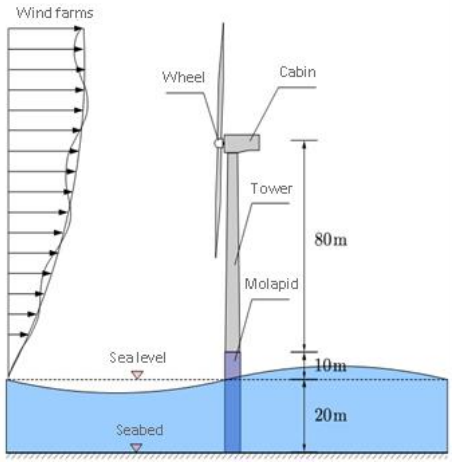

Figure 1. NREL - OC3 Wind Turbine Model Diagram

3. Wind Load

3.1 Simulation of Wind - Speed Time History

To analyze the aerodynamic response of offshore wind turbines under the action of typhoons, the wind speed is first simulated. Wind usually behaves as a disordered movement, with airflows interfering with each other to form turbulent wind. Based on a large number of statistical analyses, the turbulent wind can be divided into two parts: the mean wind and the fluctuating wind, that is

$$U(z,n) = \overline{u}(z) + u(z,n) \tag{1}$$

In the formula, *U(z,n)* represents the turbulent wind at height *z* at time n, is the mean wind at height *z*, and *u(z,n)* is the fluctuating wind at height *z* at time *n*.

3.1.1 Simulation of Wind - speed Time History

For the steady - state wind, the average wind speed is related to the height, and this relationship is usually described by the average wind profile. Prandtl was the first to derive the logarithmic - model average wind profile through the study of the turbulent boundary layer of a flat plate (Tao et al., 2024), and its expression is:

$$\overline{u}(z) = \frac{u_*}{k_*} ln\left(\frac{z}{z_0}\right) \tag{2}$$

Among them, *z* represents the height at a certain point, z_0 is the ground roughness length, which can be obtained empirically based on different terrains, is the friction velocity, and is the Karman constant. Although the logarithmic model has relatively high accuracy, in engineering practice, in order to simplify the calculation, the exponential mean wind profile model is often used, that is:

$$\overline{u}(z) = v_{ref}(\frac{z}{z_{ref}})^{\alpha} \tag{3}$$

In the formula, represents the reference height, is the average wind speed at the reference height z_{ref}, is the ground roughness index, and its value varies according to the specifications of different countries. Given that the typhoon average wind speed conforms to the exponential model within the height of 200m near the ground, this section will adopt the exponential average wind profile model to calculate the average wind speed at different heights.

3.1.2 Simulation of Fluctuating Wind

Pulsating wind is a variable that changes over time. In fact, the simulation of pulsating wind speed is equivalent to the simulation of a random process, and its statistical characteristics are generally described by the pulsating wind speed spectrum (Yang, 2020). At present, the commonly used pulsating wind speed power spectrum models include Davenport spectrum, Kaimal spectrum, Karmal spectrum, etc. In order to analyze the response of the wind turbine, the Kaimal wind speed spectrum recommended in the IEC 61400-1 specification is used for wind field simulation, and the expression is as follows:

$$\frac{fS_K(f)}{\sigma_K^2} = \frac{4fL_K/V_{hub}}{(1+6fL_K/V_{hub})^{5/3}} \tag{4}$$

Among them, *K* = *a*, b*, c** represent the wind speed components in the along - wind direction, cross - wind direction and vertical - wind direction respectively; *f* represents the frequency; represents the standard deviation of the *K* wind speed component; is the turbulence integral scale parameter, and its calculation method is given by the IEC specification, and is the average wind speed at the hub height.

In addition, when performing fluctuating wind simulations at multiple points simultaneously, considering the spatial coherence among each point, it is usually necessary to introduce a spatial coherence function. According to the IEC specification, the spatial coherence function in the along - wind direction is:

$$Coh(r_*, f) = exp\,[-12((f \cdot r_*/V_{hub})^2 + (0.12r_*/L_c)^2)^{0.5}] \tag{5}$$

r_* represents the distance between two points; is the coherence scale parameter, and its value is given by the IEC specification. After introducing the spatial coherence between each point, the cross - power spectral density function of the wind speed is:

$$S_{yj} = \sqrt{S_{yy}S_{jj}}Coh_{y,j} \tag{6}$$

Among them, represents the auto - power spectral density at the spatial point *y* (*y* = 1,2,……,*N*); is the

auto - power spectral density at j (j = 1,2,……,N), where N is the number of simulation points, and $ is the cross - correlation power spectral density function at y and j.

After obtaining the power spectrum of the fluctuating wind speed, the linear filtering method can be used to simulate the time - history of the fluctuating wind speed. The linear filtering method (Yang, 2005) is a commonly used method in stochastic process simulation, among which the autoregressive (AR) model is particularly widely used. However, in the actual wind field, in addition to the fluctuating wind speed with Gaussian characteristics, there are also wind speed fluctuations with non - Gaussian characteristics. In order to more accurately reflect the non - Gaussian characteristics in the actual wind field, this paper adopts the multivariate autoregressive (AR) model and combines it with the Johnson transformation model (JTM) to simulate the fluctuating wind speed with non - Gaussian characteristics. The AR model is expressed as:

$$X(n) = -\sum_{k=1}^{p} a_k X(n-k) + W(n) \tag{7}$$

Among them, is an N -variable non - Gaussian process, where represents its v(v=1, 2, …, N) component process. is the input process vector of N variables, and represents the non - Gaussian white noise with zero mean for the v_{th} component process; p is the order of the AR model, which can be determined by criteria such as AIC and BIC; is the k_{th} model parameter matrix of size N×N, which can be obtained from the target cross - correlation function. It is worth noting that the target cross - correlation function and the target power spectrum are Fourier transform pairs.

Once the AR model is determined, the non - Gaussian process can then be simulated based on the input non - Gaussian white noise vector. However, the statistical moment information of these non - Gaussian white noises is usually not directly obtainable, but can be deduced from the existing statistical moments of the target non - Gaussian process. This will be presented hereinafter.

The output process vector in equation (7) can also be expressed as (Ma et al., 2019).

$$X(n) = \sum_{i=0}^{\infty} h(i)\, W(n-i) \tag{8}$$

Among them, $h(i)$ is an identity impulse response matrix with a size of N×N, as shown below:

$$h(i) = \begin{bmatrix} h_{11}(i) & h_{12}(i) & \cdots & h_{1N}(i) \\ \vdots & \vdots & \ddots & \vdots \\ \vdots & \vdots & \ddots & \vdots \\ h_{N1}(i) & h_{N2}(i) & \cdots & h_{NN}(i) \end{bmatrix} \tag{9}$$

Among them, $h_{vs}(i)$(s=1,2,…,N) represents the contribution rate of the input process to the output process$x_v(n)$. According to formula (8), can be expressed as:

$$x_v(n) = \sum_{i=0}^{\infty} \sum_{s=1}^{N} h_{vs}(i) w_s(n-i) \tag{10}$$

For a stable system, generally decays to zero when the value of i is extremely large, and the decay rate depends on the transfer function of the linear system (Box et al., 1990). For broadband signals such as typical wind loads (e.g., wind speed), decays relatively fast and usually tends to zero when $i < 10000$. Consequently, when the input vector Q is input at $0 \le i \le 9999$, can be regarded as being equal to the output of the v_{th} component in the AR model, and $h_{vs}(i)$ is equal to zero when $i \ge 10000$, where Q is an N×10000 matrix, as shown below:

$$Q = \begin{bmatrix} 0 & 0 & 0 & \cdots & 0 \\ \vdots & \vdots & \vdots & \ddots & \vdots \\ 1 & 0 & 0 & \cdots & 0 \\ \vdots & \vdots & \vdots & \ddots & \vdots \\ 0 & 0 & 0 & \cdots & 0 \end{bmatrix} (s^{th} line) \tag{11}$$

Please note that except for the element in the s_{th} row and the 1_{st} column of Q being 1, all other elements in Q are equal to 0.

According to equation (10), the first four central moments of the output process vector can be estimated from the central moments of the input process vector as follows (Ma et al., 2019; Brillinger et al., 1967; Wu et al., 2020):

$$r_{X,1} = 0 \tag{12}$$

$$r_{X,2} = A_2 r_{W,2} \tag{13}$$

$$r_{X,3} = A_3 r_{W,3} \tag{14}$$

$$r_{X,4} = A_4 r_{W,4} + 3F' \tag{15}$$

Among them, $r_{X,m} = \left[r_{x_1,m}, r_{x_2,m}, \cdots r_{x_N,m}\right]^T$ and $r_{W,m} = \left[r_{w_1,m}, r_{w_2,m}, \cdots r_{w_N,m}\right]^T$, respectively represent the m_{th} order (m = 1, 2, 3, 4) central moment matrices of the output and input process vectors in the AR model, where and respectively represent the m_t order central moments of the v_{th} component processes of X(n) and W(n); for the detailed derivation processes of A_2, A_3, A_4 and $F' = \left[\frac{F_1}{r^2_{x_1,2}}, \frac{F_2}{r^2_{x_2,2}}, \cdots \frac{F_N}{r^2_{x_N,2}}\right]^T$, refer to this paper(Ma et al., 2019). Based on equations (12) - (15), the statistical moments of the non - Gaussian white noise of the input process can be inversely calculated.

According to the transfer process theory, the non - Gaussian white noise process vector W(n) can be

obtained from the underlying Gaussian white noise process vector through a nonlinear memoryless transformation (Grigoriu, 1984, 1988).

$$w_v(n) = g_v[d_v(n)] = F_{W_v}^{-1}\{\phi[d_v(n)]\} \tag{16}$$

The function is a transfer function. Here, is the cumulative distribution function (CDF) of w_v. and $F_{W_v}^{-1}$ is the inverse function of F_{W_v}. ϕ is the CDF of the standard Gaussian process.

Formula (16) is usually implicit, which causes inconvenience for non - Gaussian simulations. To simulate non - Gaussian processes more conveniently, the moment - based transformation model proposed by Johnson can relate the non - Gaussian white noise process to the underlying white noise Gaussian process $D(n)$, and is often selected as the transfer function. This model is known as the Johnson Transformation Model (JTM). According to the JTM, formula (16) can be expressed as the following three systems:

(1) system S_U

$$w_v = \varepsilon_v + \lambda_v sinh\left(\frac{d_v-\gamma_v}{\eta_v}\right) \tag{17}$$

(2) system S_B

$$w_v = \varepsilon_v + \lambda_v\left[1 + exp\left(\frac{\gamma_v-d_v}{\eta_v}\right)\right] \tag{18}$$

(3) system S_L

$$w_v = \varepsilon_v + \lambda_v exp\left(\frac{d_v-\gamma_v}{\eta_v}\right) \tag{19}$$

among them, η, γ, ε and λ are the parameters of JTM, and they can be estimated by the method of moment estimation according to the first four moments of *Wv*. The specific estimation procedure can be found in this paper (Wu et al., 2020).

In summary, by combining the AR model with the JTM model, the non - Gaussian fluctuating wind time - history at each measurement point can be generated, and it can be superimposed with the mean wind at each point, thus obtaining the turbulent wind sample.

3.2 Calculation of Wind Load

Calculate the basic wind pressure from the basic wind speed by using the following formula:

$$w_{k,z} = \frac{1}{2}\rho U_z{}^2 c_p \tag{20}$$

among them, represents the air density; is the basic wind speed at height *z*; and is the wind - load shape coefficient. In the above formula, the basic wind - pressure value does not take into account the influence of the building's shape. Regarding the calculation of the wind - load shape coefficient, there are mainly two methods: One is to make a small - scale model of the building and place it in a specially - made wind tunnel for testing, and use the pressure - measuring hole method to determine the pressure distribution on the surface of the model. The other is to measure the surface pressure distribution on the actual building, and the result obtained is that under a certain strong - wind action (Shi, 2008). In this experiment, the model was further simplified, and the standard wind - load shape coefficient was adopted, that is, =+1.0.

This article also obtains the required data based on the standards. For the convenience of calculation, according to the spirit of the standards, the following assumptions are made during the calculation:

(1) In this case, the wind - receiving components have the same wind direction;

(2) The wind force acts on the centroid of the wind - direction projection area of the wind - receiving components;

(3) When receiving the wind, the mutual shielding effect between other structures is not considered;

(4) The couple moment generated by the above forces can only cause the platform to tilt without considering the influence of the platform rotating around the Z - axis.

The force on the tower was analyzed, and the tower barrel was further simplified. The resultant force formula is as follows:

$$F = \frac{1}{2} w_{k,z=H} H d \tag{21}$$

Among them, represents the wind load; *H* stands for the height of the tower barrel; *d* is the diameter of the tower barrel. Eventually, the tower barrel bending moment is obtained:

$$M = \frac{2}{3} HF \tag{22}$$

Here, *M* is the diameter of the tower barrel; *H* is the height of the tower barrel.

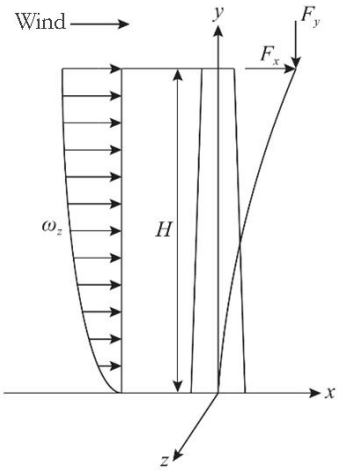

Figure 2. Schematic Diagram of Wind Load

4. Calculation of Dynamic Response

In this research, the tower barrel was simplified into a cantilever beam structure. Subsequently, the wind load was computed in accordance with the wind speed simulation outcomes at the top of the tower. After that, an analysis was carried out on the bending moment response at the bottom of the tower.

The JTM model was employed for the wind speed simulation at the top of the tower. This model was segmented into the SU area and the SB area. It was utilized to simulate various types of wind speeds. In the SU area, it simulated the strong non - Gaussian wind speed (Su, str) and the weak non - Gaussian wind speed (Su, mil). In the SB area, it simulated the strong non - Gaussian wind speed (SB, str) as well as the hardening process (SB, har) which had a kurtosis less than 3. The settings of skewness and kurtosis are presented in Table 2. The simulation results are depicted in Figures 3 - 6. Evidently, the wind speed time - histories in each situation exhibit remarkable non - Gaussian characteristics.

It should be noted that this method of simplifying the tower barrel into a cantilever beam structure is a common approach in relevant studies. It allows for a more straightforward analysis of the structural response under wind load. Moreover, the accurate simulation of different wind speeds in different areas is crucial for understanding the overall impact on the tower structure.

Table 2. Skewness and Kurtosis Values of Fluctuating Wind Speed in Numerical Cases

Case	Skewness	Kurtosis
Su, str	-1.59	8.63
Su, mil	-0.64	3.96
$S_{B,}$ *str*	-2.17	11.55
$S_{B,}$ *har*	-0.40	2.69

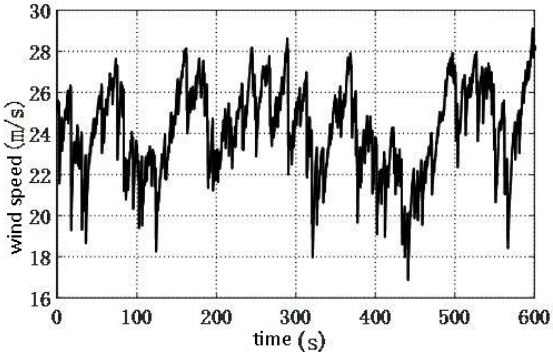

Figure 3. The Time - history of the Wind Speed at the Pinnacle of the Tower (*Su, str*)

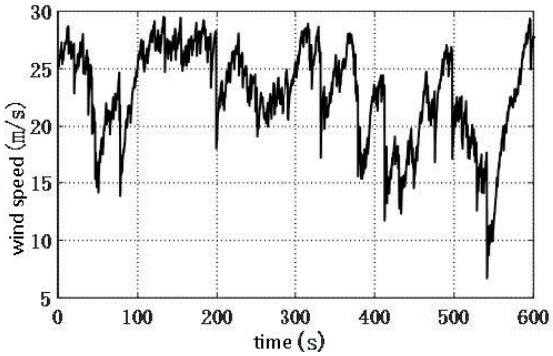

Figure 4. The Time - History of the Wind Speed at the Pinnacle of the Tower (*Su, mil*)

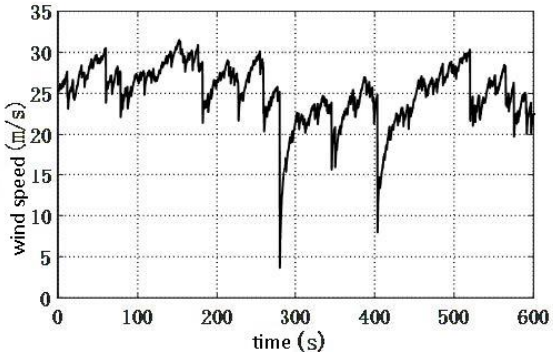

Figure 5. The Time - History of the Wind Speed at the Pinnacle of the Tower (S_B, *str*)

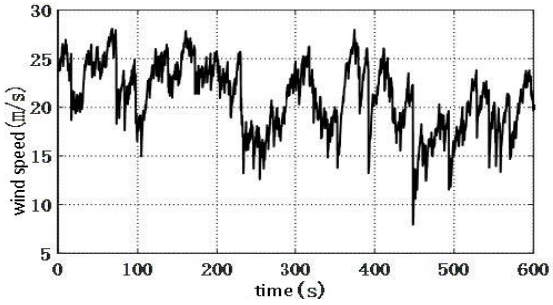

Figure 6. The Time - History of the Wind Speed at the Pinnacle of the Tower (S_B, *har*)

Utilizing the simulated wind speed, the wind load is computed in accordance with the formula, and subsequently, the bending moment diagram at the base of the tower is acquired. The time - history of the bottom - of - tower bending moment is presented in Figures 7 - 10. It is evident that the wind - induced responses of the wind turbines in each scenario exhibit distinct non - Gaussian characteristics.

Based on this time - history, the first four - order moments, namely the mean, standard deviation, skewness, and kurtosis of the wind - induced responses, can be determined and are tabulated in Table 3. It should be noted that while there is no entirely strict positive correlation, in the majority of cases, the more significant the deviation of the wind speed skewness is, the more significant the deviation of the wind turbine response skewness will be as well, and they are in the same direction (both being negative skewness). Moreover, the larger the wind speed kurtosis is, the greater the wind turbine response kurtosis will be. When the wind speed is a hardening process, the non - Gaussian property of the wind turbine response is less pronounced.

In addition, it is important to understand that these relationships play a crucial role in the overall analysis of wind turbine performance. The accurate determination of these relationships helps in predicting the behavior of wind turbines under different wind conditions more precisely. This, in turn, can lead to better design and maintenance strategies for wind turbines, ensuring their long - term efficiency and reliability in the field.

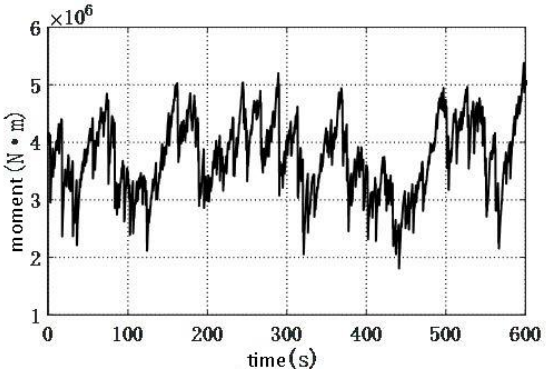

Figure 7. The Time - History of Bending Moment at the Bottom of the Tower (*Su, str*)

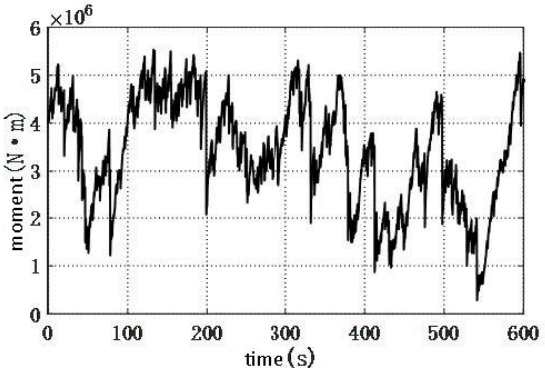

Figure 8. The Time - History of Bending Moment at the Bottom of the Tower (*Su, mil*)

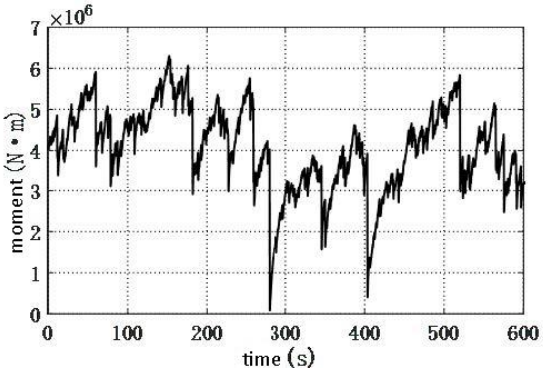

Figure 9. The Time - History of Bending Moment at the Bottom of the Tower (S_B, *str*)

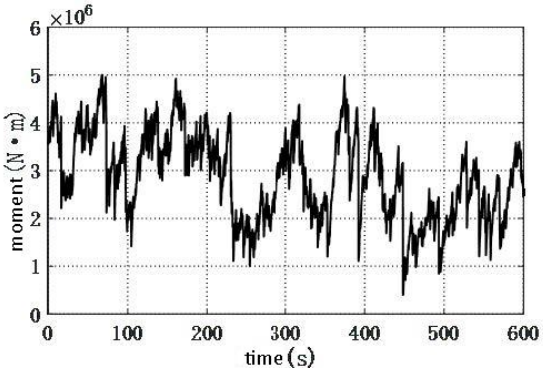

Figure 10. The Time - History of Bending Moment at the Bottom of the Tower (S_B, *har*)

Table 3. The First Four - Order Statistical Moments of the Wind Turbine Response

Case	Case Mean (*kN·m*)	Standard Deviation (*kN·m*)	Skewness	Kurtosis
Su, str	3730.2	646.6	-1.59	8.63
Su, mil	3410.0	1127.4	-0.64	3.96
$S_{B,}$ *str*	4069.4	1025.6	-2.17	11.55
$S_{B,}$ *har*	2871.2	904.7	-0.40	2.69

3. Conclusion

This article has carried out research regarding the response characteristics of wind turbine structures when subjected to typhoon non - Gaussian wind loads. Moreover, it has comprehensively analyzed the response characteristics of wind turbine structures under non - Gaussian wind loads of varying intensities. The following principal conclusions have been reached:

(1) The non - Gaussian wind field simulation method founded on AR - JTM is capable of more precisely and effectively simulating the non - Gaussian wind field. For instance, in comparison to some traditional simulation methods, it can better capture the complex characteristics of non - Gaussian wind

fields, which is crucial for accurately predicting the behavior of wind turbine structures in such conditions.

(2) The more pronounced the deviation of the wind speed skewness, the more notable the deviation of the wind turbine response skewness will be, and they are in the same direction (both are negatively skewed). Additionally, as the wind speed kurtosis increases, so does the wind turbine response kurtosis. That is to say, the stronger the non - Gaussian characteristics of the wind field, the more powerful the non - Gaussian characteristics of the wind turbine response. Consider a scenario where the wind field has extremely high non - Gaussian characteristics due to certain geographical or meteorological factors. In this case, the wind turbine response will also exhibit highly non - Gaussian characteristics, which may pose greater challenges to the stability and safety of the wind turbine.

(3) Whether it is the wind speed or the wind turbine response, the skewness and kurtosis under strong non - Gaussian conditions are greater than those under weak non - Gaussian conditions. This implies that the data distribution under strong non - Gaussian conditions drifts further away from the normal distribution and possesses more robust non - Gaussian characteristics. For example, in a strong non - Gaussian wind environment, the data points of wind speed and wind turbine response may be more scattered and deviate significantly from what would be expected in a normal distribution, which requires more advanced analysis and design considerations for wind turbines.

(4) When the wind speed is a hardening process, the non - Gaussian nature of the wind turbine response is relatively feeble, as manifested by a skewness close to 0 and a lower kurtosis. This situation may be related to the physical mechanisms within the wind turbine system during the hardening process of wind speed. It could be that certain internal components or control systems of the wind turbine play a role in reducing the non - Gaussian nature of the response, but further research is needed to fully understand this phenomenon.

References

Bai, Q. (2005). *Numerical Simulation Research on Wind Speed Time - history*. Liaoning: Northeastern University.

Box, G. H. P., & Jenkins, G. M. (1990). *Time Series Analysis, Forecasting, and Control. Holden - Day*.

Brillinger, D. R., & Rosenblatt, M. (1967). *Computation and Interpretation K_{th} Order Spectra*.

Grigoriu, M. (1984). Crossings of Non - Gaussian Translation Processes. *J. Eng. Mech*, *110*(4), 610-620. https://doi.org/10.1061/(ASCE)0733-9399(1984)110:4(610)

Grigoriu, M. (1998). Simulation of Stationary Non - Gaussian Translation Processes. *J. Eng. Mech.*, *124*(2), 121-126. https://doi.org/10.1061/(ASCE)0733-9399(1998)124:2(121)

Huang, B. C. (2001). *Principles and Applications of Wind - resistant Structure Analysis*. Shanghai: Tongji University Press.

International Electrotechnical Commision (IEC). (2009). *Wind Turbines - part 1: design requirements: IEC 61400 - 1*.

Li, B., Wen, H. T., & Gong, Z. R. (2017). Research on Wind - induced Response Analysis and Wind - vibration Control of Wind Turbine Tower. *Engineering Mechanics*, *34*(S1), 134-138.

Liu, D. S., Dai, J. C., Hu, Y. P. et al. (2013). *Current Situation and Development Trend of Modern Large - scale Wind Turbine Units*, *24*(1), 125-135.

Lobitz, D. W. (1984). *A Nastran - based Computer Program for Structural Dynamic Analysis of Horizontal Axis Wind Turbines*. Sandia National Laboratories.

Ma, X. L., & Xu, F. Y. (2019). An Efficient Simulation Algorithm for Non - Gaussian Stochastic Processes. *Journal of Wind Engineering and Industrial Aerodynamics: The Journal of the International Association for Wind Engineering*, *194*. https://doi.org/10.1016/j.jweia.2019.103984

Miao, S., & Jin, H. F. (2021). Estimation of Extreme Response of Wind Turbine Structures under Non - Gaussian Wind Field. *Building Structure*, *51*(S2), 253-258.

Murtagh, P. J., Basu, B., & Broderick, B. M. (2008). Along - wind Response of a Wind Turbine Tower with Blade Coupling Subjected to Rotationally Sampled Wind Loading. *Engineering Structures*, *27*(8), 1209-1219. https://doi.org/10.1016/j.engstruct.2005.03.004

Murtagh, P. J., Collins, R., Basu, B. et al. (2004). Dynamic Response and Vibration Control of Wind Turbine Towers. *Irish Engineers Journal*, *58*(7), 1-7.

Quan, Y. (2002). *Research on Cross - wind Load and Response of Super - high - rise Buildings*. Tongji University.

Shi, J. (2008). *Research on Wind Load Calculation on Offshore Platforms*. Liaoning: Dalian University of Technology.

Tao, Z., Ma, Y., You, R. Q. et al.(2024). Review of Research Progress in Boundary Layer Theory. *Scientia Sinica (Technologica)*, *54*(6), 979-1002. https://doi.org/10.1360/SST-2023-0316

Wang, J. P. (2007). Simulation of Multi - dimensional Fluctuating Wind Load Time - history Based on AR Model Method. *Journal of Guizhou University (Natural Science Edition)*, *2007*(5), 526-529.

Wang, Z., Zhao, Y., Li, F. et al. (2013). Extreme Dynamic Responses of MW - level Wind Turbine Tower in the Strong Typhoon Considering Wind - rain Loads. *Mathematical Problems in Engineering. https://doi.org/10.1155/2013/512530*

Wu, F. B., Huang, G. Q., Liu, M., & Peng, L. L. (2020). Sampling Error Comparison Study of Non - Gaussian Wind Pressure Extreme Value Estimation: Moment - based Transformation Process Method. *Journal of Vibration and Shock*, *39*(18), 20-26+43.

Wu, F., Huang, G., & Liu, M. (2020). Simulation and Peak Value Estimation of Non - Gaussian Wind Pressures Based on Johnson Transformation Model. *J. Eng. Mech*, *146*(1), 04019116. https://doi.org/10.1061/(ASCE)EM.1943-7889.0001697

Yang, J. H. (2020). *Research on Along - wind Vibration Response and Equivalent Wind Load of High - rise / High - rise Structures*. Zhengzhou: Zhengzhou University.

Zhang, X. W., & Wen, W. (2013). Research on Dynamic Response Characteristics of Large - scale Wind Turbine Towers under Fluctuating Wind. *Journal of Sichuan University of Science &*

Engineering (Natural Science Edition), *26*(2), 32-35.

Zhao, Y. (2018). *Research on Structural Vibration Monitoring and Dynamic Response of Wind Turbines*. Zhejiang University.